Density Standard at NMIJ and Related Activities in the CCM WG on Density

Kenichi Fujii [*] and Mitsuru Tanaka

National Metrology Institute of Japan, AIST Central 3, Tsukuba, Ibaraki 305-8563, Japan
[*]E-mail: fujii.kenichi@aist.go.jp

The Avogadro constant is one of fundamental physical constants used in physics and chemistry. In metrology, its accurate value is of primary importance for realizing a new definition of the kilogram, the last SI base unit still defined by the material artifact. For the determination of the Avogadro constant by the x-ray crystal density (XRCD) method, the National Metrology Institute of Japan (NMIJ) developed an optical interferometer to measure the diameters of a single-crystal silicon sphere, and succeeded in determining the density with a relative standard uncertainty of 1×10^{-7}. From a differential density measurement, the density of any other silicon crystals can be calibrated with a relative standard uncertainty of a few parts in 10^7. A new magnetic suspension density meter was developed at the NMIJ, where the silicon crystal is used as a sinker. Since the thermal expansion coefficient and elastic constants of silicon crystals are well known with small uncertainties, $p\rho T$ properties of fluids may be determined with a relative standard uncertainty of a few parts in 10^6. Using the silicon density standard, some of the National Metrology Institutes (NMIs) have started a new absolute measurement for the density of water. These results are being discussed at the Working Group (WG) on Density, organized by the Consultative Committee for Mass and Related Quantities (CCM) of the International Committee for Weights and Measures (CIPM). Recent progress at the NMIJ and related activities in the CCM WG on Density are presented.

1. Introduction

In the International System of Units (SI) [1], the unit of density (kg m^{-3}) is derived from the two SI base units: the unit of mass, the kilogram, and the unit of length, the metre. When determining the absolute value of the density, the measurement should therefore be traceable both to the mass standard defined by the international prototype of the kilogram [2, 3] and to the length standard referred to the wavelength of lasers stabilized at recommended radiations [4]. In practice, the absolute measurement consists of absolute mass and volume measurements of a solid object whose volume can be related to the length standard with a small uncertainty. Recent strategies for determining the volume from length measurement use a sphere because a sphere is much less susceptible to be damaged than a cube or a cylinder, and current fabrication technologies supply spheres of excellent sphericities.

The absolute measurement of the density using a sphere was first realized at the National Institute of Standards and Technology (NIST) in 1972 [5, 6] for a determination of the Avogadro constant, N_A, by the x-ray crystal density (XRCD) method, where absolute measurements of the lattice constant a, density ρ, and molar mass M of an identical silicon crystal are performed. Since a silicon crystal has cubic symmetry with eight atoms in a unit cell, N_A is obtained as

$$N_A = 8M/(\rho a^3). \tag{1}$$

The determination of N_A by the XRCD method, which was pioneered by Deslattes and co-workers [7, 8] in the

1970s, imposed a huge influence on the density standard. In 1987, a new technique for polishing a 1-kg silicon sphere was developed at the CSIRO [9, 10]. This technique enabled us to realize a new solid density standard directly traceable to the mass and length standards. Optical interferometers have therefore been developed at NMIs to reduce the uncertainty in the density measurement.

2. Absolute density measurement

2.1. Volume of an approximate sphere Figure 1 shows the interferometer developed at the NMIJ [11, 12]. The
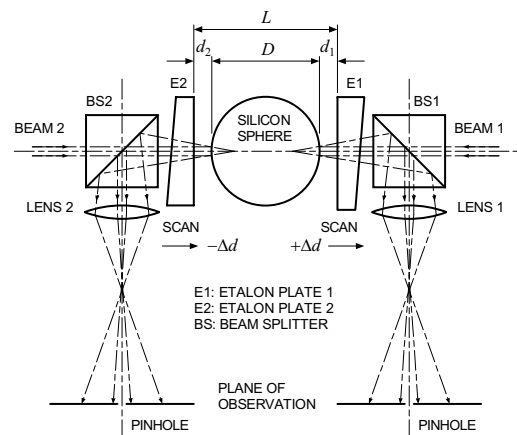

Fig. 1. Principle of the diameter measurement using a scanning-type optical interferometer [11, 12].

silicon sphere is placed in a Fabry-Perot etalon of known plate separation, L, and a light beam from a frequency-stabilized laser is set with normal incidence to each of the etalon plates. Interference fringes are produced by the light beams reflected from the etalon plate E1 and the adjacent surface of the sphere. An analysis of the concentric circular fringes produced at the plane of observation determines the gap, d_1, between the sphere and the etalon plate E1. Similar fringes are produced for the other side of the sphere, and the same analysis determines the gap, d_2, between the sphere and the etalon plate E2. The diameter of the sphere, D, is given by

$$D = L - (d_1 + d_2). \quad (2)$$

Figure 2 shows a geometrical consideration when the diameter of an approximate sphere is measured by the optical interferometer with two parallel etalon plates. As can be seen from the figure, this interferometer measures a breadth of the sphere instead of a diameter. Since the breadth is equal to or larger than the diameter which passes through a gravity center O, this causes a systematic difference in determining a true volume of an approximate sphere [13]. When the distance from O to one of the parallel planes is denoted by p, and its mean over the surface of the sphere is denoted by p_0, the spherical harmonics, $Y_n = p - p_0$, are expressed as

$$Y_n(\theta,\phi) = \sum_{m=0}^{n} \left[(A_{nm} \cos m\phi + B_{nm} \sin m\phi) \cdot P_n^m(\cos\theta) \right] \quad (3)$$

where θ and ϕ are azimuthal and polar angles expressed in spherical coordinates, respectively, A_{nm} and B_{nm} the amplitudes of spherical harmonics of degree n and order m, and P_n^m the associated Legendre function. The volume of the approximate sphere, V, is then calculated as

$$V = \frac{4}{3}\pi p_0^3 - \frac{1}{2} p_0 \sum_{n=2}^{\infty} \left[(n-1)(n+2) \int_0^{2\pi} \int_0^{\pi} Y_n^2 \sin\theta \cdot d\theta \cdot d\phi \right]. \quad (4)$$

For example, if we consider an approximate sphere of a mean breadth of 100 mm with tetrahedral symmetry of a peak-to-valley radial deviation of 1 μm, the relative
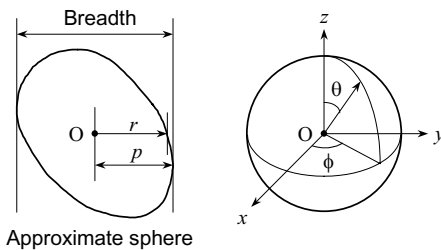
contribution, $\Delta V/V$, of the second term on right hand side of equation (4) is 1×10^{-9}. When the peak-to-valley radial deviation is 100 nm, it further reduces to 1×10^{-11}, showing that the volume of an approximate sphere may be determined with a very small uncertainty by measuring the breadths along many directions. For convenience, we refer to the breadth as the diameter in the following sections.

2.2. Optical interferometer Figure 3 shows an experimental setup for the diameter measurement [14]. A frequency-stabilized He-Ne laser is used as a primary light source. The frequency of the laser is referred to that of an iodine-stabilized He-Ne laser [4]. The two intensities I_1 and I_2 are detected by photodetectors, and then amplified by lock-in amplifiers. The sphere and the etalon are placed in a vacuum chamber to eliminate the uncertainty due to the refractive index of air. A platinum resistance thermometer is inserted in a copper block placed near the etalon. A small temperature difference between the etalon and the copper block is detected by thermocouples.

The direction of the sphere is changed by a rotation mechanism installed under the sphere. A spherical harmonic function is used to calculate the mean diameter D_m [15]. The volume of the silicon sphere is then obtained as $V = \pi D_m^3/6$.

Recent technologies in laser diodes extended the

Fig. 2. Geometrical consideration to determine the volume of an approximate sphere [13].
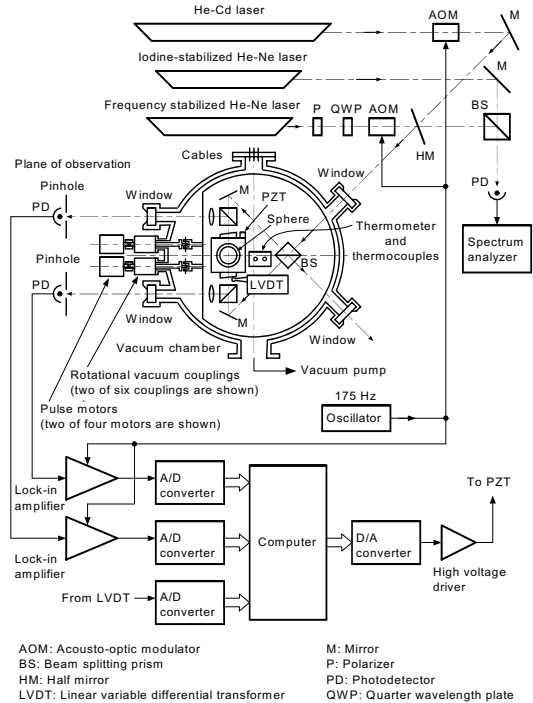

Fig. 3. Experimental setup of the interferometer for measuring diameters of a silicon sphere in a vacuum [14].

tunable range of optical frequencies. They are so convenient to use as a light source that recent interferometers [16] use the phase-shifting method to measure the fractional order of interference. The dimensional measurement of silicon spheres is thus replaced by optical frequency measurements.

2.3. Ellipsometry Since the surface of the silicon sphere is covered by a natural oxide layer, the effect of phase retardation on reflection at the oxide layer causes a systematic difference between the observed and real diameters when it is measured by the optical interferometer described earlier.

Figure 4 shows schematically a structure near the surface of the silicon sphere. When the refractive indices of a vacuum and the oxide layer are denoted by n_0 and n_1, respectively, the amplitude reflection coefficient r_{01} at the interface between the vacuum and the oxide layer is given by [17]

$$r_{01} = \frac{n_0 - n_1}{n_0 + n_1}. \qquad (5)$$

When the complex refractive index of the silicon crystal is denoted by $N_2 = n_2 - ik_2$, the amplitude reflection coefficient r_{12} at the interface between the oxide layer and the substrate is given by

$$r_{12} = \frac{n_1 - N_2}{n_1 + N_2} = \frac{n_1^2 - n_2^2 - k_2^2 + i2n_1k_2}{(n_1 + n_2)^2 + k_2^2} = |r_{12}|e^{i\phi_{12}}, \qquad (6)$$

where

$$|r_{12}| = \sqrt{\frac{(n_1 - n_2)^2 + k_2^2}{(n_1 + n_2)^2 + k_2^2}}, \text{ and} \qquad (7)$$

$$\phi_{12} = \tan^{-1}\left(\frac{2n_1k_2}{n_1^2 - n_2^2 - k_2^2}\right). \qquad (8)$$

The total reflection coefficient, R, including the effect

Incident light beam

$n_0 = 1$

SiO$_2$
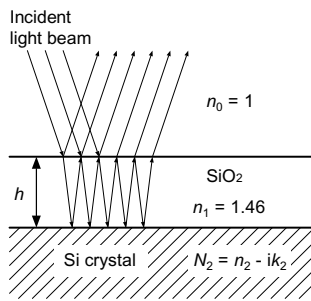
h

$n_1 = 1.46$

Si crystal $N_2 = n_2 - ik_2$

Fig. 4. A model showing a structure near the surface of the silicon sphere covered by an oxide layer with a thickness h [19].

of multiple reflections in the oxide layer, is therefore given by

$$R = \frac{r_{01} + r_{12}e^{-i2\beta}}{1 + r_{01}r_{12}e^{-i2\beta}} = \frac{r_{01} + |r_{12}|e^{i(\phi_{12}-2\beta)}}{1 + r_{01}|r_{12}|e^{i(\phi_{12}-2\beta)}} = |R|e^{i\delta}, \qquad (9)$$

where $\beta = 2\pi hn_1/\lambda_0$, λ_0 is the wavelength in a vacuum,

$$|R| = \sqrt{\frac{r_{01}^2 + |r_{12}|^2 + 2r_{01}|r_{12}|\cos(\phi_{12} - 2\beta)}{1 + r_{01}^2|r_{12}|^2 + 2r_{01}|r_{12}|\cos(\phi_{12} - 2\beta)}}, \text{ and} \qquad (10)$$

$$\delta = \tan^{-1}\left[\frac{|r_{12}|(1 - r_{01}^2)\sin(\phi_{12} - 2\beta)}{r_{01}(1 + |r_{12}|^2) + |r_{12}|(1 + r_{01}^2)\cos(\phi_{12} - 2\beta)}\right]. \qquad (11)$$

Equation (11) gives the total phase retardation δ on reflection at the surface of the oxide layer. To calculate δ, the thickness h is usually measured by ellipsometry [18] with input parameters $\lambda_0 = 633$ nm, $n_0 = 1$, $n_1 = 1.46$, $n_2 = 3,88$, and $k_2 = 0.019$ [19].

The results have shown that the thickness h is usually about 5 nm for silicon spheres polished at the CSIRO. When the diameter is measured with a light source of 633 nm wavelength, $(\delta - \pi)$ is about 0.1 rad. This means that the real diameter is larger than the observed one by about 10 nm. The density of the silicon sphere may be determined from the mass and volume including the oxide layer because the density of the oxide layer is close to that of silicon crystals.

2.4. Mass measurement Since the masses of these silicon spheres are so close to 1 kg, a direct comparison with a 1-kg standard weight can be provided. However, the volume difference between the silicon sphere and the stainless steel weight causes a large difference in buoyancy forces of air when the mass is measured in air. To overcome the difficulty, a sinker system was used at NMIJ directly to measure the density of air, where a set of 1-kg stainless steel weights of nearly the same surface areas but different volumes are alternately weighed in air [20]. At the NMIJ, the masses of the 1-kg silicon spheres have been determined with a combined standard uncertainty of 17 μg [21].

2.5. Density Table 1 lists the uncertainty sources in the absolute measurement of the density of silicon spheres. The densities of two silicon spheres, designated as S4 and S5, were determined at 22.5 °C and 0 Pa. As can be seen in this table, the largest uncertainty source lies in the random component in the volume determinations, where a single volume is determined from 70 diameter measurements, and the volume determination was repeated three times for each of the two spheres. The second largest uncertainty source lies in the uncertainty of the temperature measurements. The relative

combined standard uncertainties in their densities at 22.5 °C and 0 Pa are thus estimated to be 0.65×10^{-7} and 1.08×10^{-7} for S4 and S5, respectively [21].

In order to determine the density at 20 °C and 101.325 kPa, which is referred to as a standard state, they were corrected for the pressure using elastic constants of silicon crystals [22, 23] and for the thermal expansion [24, 25]. The densities at 20 °C and 101.325 kPa were thus determined with relative combined standard uncertainties of 0.99×10^{-7} and 1.32×10^{-7} for S4 and S5, respectively. The silicon spheres are presently used as a primary density standard at the NMIJ.

3. Differential density measurement

3.1. Hydrostatic weighing Figure 5 shows a hydrostatic weighing system that measures the density of a solid sample [26, 27]. At the NMIJ, the two silicon spheres S4 and S5 are used as the reference density standards. In this apparatus, tridecane (n-C$_{13}$H$_{28}$, $\rho \cong 756$ kg/m^3 at 20 °C) is used as a working liquid, in which the two silicon spheres and the solid sample under study are weighed alternately by an electronic balance using a weight exchange mechanism. The two silicon spheres are used to cancel the effect of any vertical density gradient in the working liquid, which may be introduced by the temperature gradient and the gravity. The two silicon spheres and the solid sample are held in a cage, and they are independently placed on and removed from the cage in the working liquid by the weight exchange mechanism. As long as the level of the working liquid is kept constant during the weight exchange, the buoyancy force acting on the cage can be canceled.

When S4 is weighed in the liquid, its apparent mass in the liquid is about 676 g because of the buoyancy force acting on the sphere. To operate the balance near 1 kg, a set of stainless steel weights with a mass of 324 g is placed on the balance pan with an automatic handler. In this state, the balance reading, B_{S4}, being a difference

from 1 kg, is recorded. The sphere and the set of weights are then removed from the balance, and a 1-kg stainless steel weight is placed on the balance pan with the automatic handler. In this state, the balance reading, B_0, being a difference from 1 kg, is recorded. The forces acting on this system are summarized as

$$m_{S4}\, g_{S4} - \rho_{liq,S4}(t)V_{S4}(t)g_{S4} + m_{324}\, g_{bal}$$
$$- \rho_{air}(t_{air})V_{324}(t_{air})g_{bal} - KB_{S4}\, g_{bal}$$
$$= m_{1000}\, g_{bal} - \rho_{air}(t_{air})V_{1000}(t_{air})\, g_{bal} - KB_0\, g_{bal}\,, \quad (12)$$

where m_{S4}, m_{324}, and m_{1000} are the masses of the sphere S4, 324-g weights, and 1-kg weight, respectively, $\rho_{liq,S4}(t)$ and $\rho_{air}(t_{air})$ the density of the working liquid near the silicon sphere S4 at temperature t and density of air at temperature t_{air}, respectively, $V_{S4}(t)$ the volume of S4 in the working liquid at temperature t, $V_{324}(t_{air})$ and $V_{1000}(t_{air})$ the volumes of the 324-g and 1-kg weights at temperature t_{air}, respectively, g_{S4} and g_{bal} the local accelerations due to gravity at the positions of the silicon sphere S4 and the balance, respectively, and K the balance sensitivity. Since the vertical distance between the balance and the sphere S4 is about 1 m, the gravity gradient coefficient, $C = g_{bal}/g_{S4}$, is estimated to be about 0.999 9997.

From Eq. (12), the liquid density near S4, $\rho_{liq,S4}(t)$, is determined. When the sphere S5 is weighed in the liquid, the liquid density near S5, $\rho_{liq,S5}(t)$ is determined in the same way. The liquid density near a solid sample, A, is determined, assuming that any vertical density gradient in the liquid is linear, with

$$\rho_{liq,A}(t) = \lfloor \rho_{liq,S4}(t) + \rho_{liq,S5}(t) \rfloor / 2 \,. \quad (13)$$

When a 1-kg silicon sample, A, with a mass of m_A is weighed in the liquid, its volume, $V_A(t)$, at temperature t

Table 1. Uncertainty sources of the absolute density measurements of the silicon spheres S4 and S5 at 22.500 °C and 0 Pa.

| Uncertainty source	Standard uncertainty	$10^7 \Delta\rho/\rho$	
		S4	S5
Uncertainty caused by random effects			
Type A evaluation			
Standard deviation of the mean		0.367	0.940
Uncertainty caused by systematic effects			
Type A evaluation			
Wavelength in vacuum ($\Delta\lambda_0/\lambda_0$)	2.3×10^{-9}	0.069	0.069
Type B evaluation			
Sphere temperature	0.005 ℃	0.387	0.387
Thickness of oxide layers	1.0 nm	0.320	0.320
Linear thermal expansivity of Si	1×10^{-8} K^{-1}	0.077	0.038
Phase shift in light propagation	0.15 mrad	0.006	0.006
Alignment of light beams	0.01 mrad	0.001	0.001
Mass	16.9 µg	0.169	0.169
Relative combined standard uncertainty		0.653	1.082
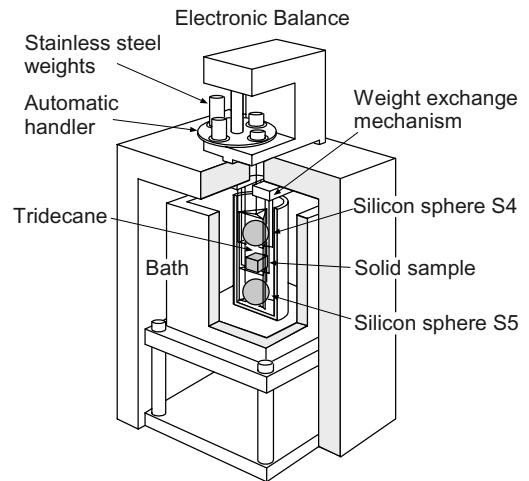
Fig. 5. Hydrostatic weighing method for comparing the densities of solid samples [26, 27].

is determined from the balance reading. The density of the sample at temperature t is thus determined as

$$\rho_A(t) = m_A/V_A(t). \qquad (14)$$

The density of the sample under study is thus compared with those of the reference silicon spheres. This system is presently used at the NMIJ for calibrating the density of other silicon crystals and solid samples, such as stainless steel weights, glasses, and metals.

The relative combined standard uncertainty in the density measurement by this hydrostatic weighing system is estimated to be 0.16×10^{-6} for 1-kg silicon crystals and 1.23×10^{-6} for 1-kg stainless steel weights when the covariance and the long term stability of the two silicon density standards are taken into account. The combined standard uncertainty in measuring the relative difference between the densities of 1-kg silicon samples is estimated to be as small as 4.5×10^{-8} [21].

3.2. Pressure-of-flotation method It is possible to measure very small differences between the densities of silicon crystals by application of pressure. This principle is called the pressure-of-flotation method [28-30]. As shown in Fig. 6, the density of an approximately 2:1 mixture of 1,2,3-tribromopropane ($\rho \cong 2410$ kg/m^3 at 20 °C) and 1,2-dibromoethane ($\rho \cong 2180$ kg/m^3 at 20 °C) contained in a closed cell is adjusted to be nearly that of silicon crystals ($\rho \cong 2329$ kg/m^3 at 20 °C) by changing the composition of the mixture. When the temperature of the liquid is uniform, a vertical density gradient occurs in the liquid because the lower liquid is compressed by its own mass under the presence of gravity, and therefore the silicon crystal may be kept in a
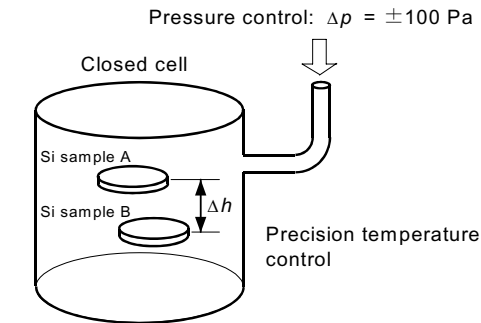
stable flotation when the density of the liquid is approximately equal to that of the silicon crystal. In such a cell, the liquid density difference in the cell for a finite height difference, Δh, is given by $\Delta\rho/\rho = \kappa_T \Delta p$, where κ_T is the isothermal compressibility of the liquid, $\Delta p = \rho g \Delta h$, and g the acceleration due to gravity. Since κ_T of the liquid is about 4.39×10^{-10} Pa^{-1} and that of silicon crystals is only 1.023×10^{-11} Pa^{-1}, the density change of silicon crystals due to a pressure change is much less than that of the liquid. This means that the pressure inside the cell may be varied so that the density of the liquid is equal to one of the silicon crystals. When the pressure difference, Δp, which is required to levitate the two silicon crystals at the same vertical position, is measured, the relative difference in the densities of the two silicon crystals may be given by

$$\Delta\rho/\rho = \kappa_T \Delta p = \kappa_T \rho g \Delta h. \qquad (15)$$

For example, the relative density difference is 1×10^{-7} when Δh is about 10 mm. It further reduces to 1×10^{-8} when Δh is about 1 mm.

This method, however, requires a very careful arrangement for temperature control. When the pressure of the liquid is changed, the initial temperature change is almost adiabatic. Therefore the liquid temperature increases by a few mK when the pressure is increased by 100 Pa. When the temperature of the closed cell is controlled in a thermal bath, the liquid temperature then decreases until thermal equilibrium is reached. Since the bulk thermal expansion coefficient of the liquid is as large as 8.6×10^{-4} K^{-1}, the liquid density change due to the temperature change is not negligible. Usually a few hours are needed before a good thermal equilibrium is obtained. A very precise temperature control is needed for a single set of density comparisons, usually requiring a temperature stability of ± 100 μK or better.

3.3. Magnetic suspension method In order to measure the $p\rho T$ properties of fluids, a new principle using a magnetic suspension was developed by Beams and Clarke [31] in 1962. Details on this principle are given elsewhere [32]. In 1986, this method was improved by Kleinrahm and Wagner [33], where a weight exchange mechanism that can be operated in a high-pressure cell was installed. Feedback control of the current in the suspension coil levitates a sinker placed on a bearing cone. When the vertical position of the magnetic levitation is changed, the bearing cone acts as a weight exchange mechanism. The electronic balance measures the buoyancy force acting on the sinker. In this method, the permanent magnet is used only for levitating the system in the high-pressure cell, and a cylinder made of titanium, glass, or tantalum has been used as the sinker.

At the NMIJ, as shown in Fig. 7, a silicon crystal is used as the material of the sinker [34] because its thermal expansion coefficient is already know accurately in a wide temperature range, and the correction for the

Pressure control: $\Delta p = \pm 100$ Pa

Closed cell

Si sample A

Si sample B Δh

Precision temperature control

2:1 mixture of 1,2,3-tribromopropane and 1,2-dibromomethane: ρ = 2329 kg·m^{-3}

Δh = 10 mm : $\Delta\rho/\rho$ = 0.117 x 10^{-6}
Δh =   1 mm : $\Delta\rho/\rho$ = 0.012 x 10^{-6}

Required temperature stability: $< \pm 100$ μK

Fig. 6. Principle of the pressure-of-flotation method developed for comparing the densities of silicon crystals.
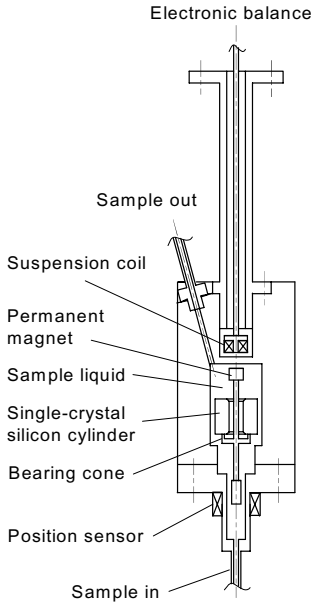
Fig. 7. Magnetic suspension densimeter developed at the NMIJ [34]. A single-crystal silicon cylinder is used as the sinker.

pressure can be evaluated accurately from its elastic constants. Its density can be calibrated either by the hydrostatic weighing method or by the pressure-of-flotation method. The density of a 60-g single-crystal silicon cylinder was determined with a relative combined standard uncertainty of 0.7×10^{-6}. This instrument is presently used at the NMIJ for measuring the density of standard liquids used for calibrating vibrating-tube densimeters. A relative combined uncertainty of 4×10^{-6} has been achieved for the density measurements of 2,2,4-trimethylpentane (*iso*-octane) at 20 °C and 101.325 kPa.

When this method is used to measure the density of fluids, the effect of magnetic properties of fluids under study is not negligible. Most of organic fluids have diamagnetic properties, and the effect due to the magnetic susceptibility of the fluids must be taken into account to accurately measure the buoyancy force [34].

4. Density of water

The earliest measurement of the density of water was performed at the Bureau International des Poids et Mesures (BIPM) [35-37] by hydrostatic weighing, where the density of water distilled from a spring near the BIPM was measured. The value thus determined by Guillaume [38] in 1927 for water at 4 °C and 101.325 kPa is 999.972 kg/m³. Since the existence of isotopes had not been discovered at that time, the value is, however, considered to have a relative standard uncertainty of about 4×10^{-6} [39]. There are four major species of water molecules: $H_2{}^{16}O$, $H_2{}^{17}O$, $H_2{}^{18}O$, and

$HD^{16}O$. Their isotopic compositions are described in terms of amount-of-substance ratios $R_D = n(D)/n(H)$, $R_{18} = n({}^{18}O)/n({}^{16}O)$, and $R_{17} = n({}^{17}O)/n({}^{16}O)$, where $n(X)$ represents the amount of substance of a nuclide X. These ratios can be determined by mass spectrometry.

4.1. Standard Mean Ocean Water (SMOW) To compare the isotopic compositions of water samples on a reliable basis, Craig [40] introduced the concept of Standard Mean Ocean Water (SMOW), that serves as a standard for reporting isotopic compositions of natural water samples. They are usually expressed by relative differences from that of SMOW:

$$\delta D = [R_D(\text{sample})/R_D(\text{SMOW}) - 1] \times 10^3, \quad (16)$$
$$\delta^{18}O = [R_{18}(\text{sample})/R_{18}(\text{SMOW}) - 1] \times 10^3, \quad (17)$$
$$\delta^{17}O = [R_{17}(\text{sample})/R_{17}(\text{SMOW}) - 1] \times 10^3, \quad (18)$$

where the approximate values for SMOW are [40-42]

$$R_D(\text{SMOW}) = (155.76 \pm 0.05) \times 10^{-6}, \quad (19)$$
$$R_{18}(\text{SMOW}) = (1993.4 \pm 2.5) \times 10^{-6}, \quad (20)$$
$$R_{17}(\text{SMOW}) = 371.0 \times 10^{-6}. \quad (21)$$

In Eq. (18), the abundance of ${}^{17}O$ is seldom measured; it is usually deduced from the following relationship for natural water [43]:

$$\delta^{17}O = 0.4989 \cdot \delta^{18}O \cong \delta^{18}O/2. \quad (22)$$

Therefore, if δD and $\delta^{18}O$ are specified, the isotopic composition of water is identified completely. Using δD and $\delta^{18}O$, the difference in the density of water from that of SMOW may be given by [44]

$$(\rho_{\text{water}} - \rho_{\text{SMOW}})/(\text{kg m}^{-3}) = 0.233 \times 10^{-3}\, \delta^{18}O$$
$$+ 0.0166 \times 10^{-3}\, \delta D, \quad (23)$$

where ρ_{water} is the density of water having isotopic compositions expressed by Eqs. (16) and (17), and ρ_{SMOW} is the density of SMOW.

SMOW is now used as a liquid density standard because the density of water with another isotopic composition can be derived from Eq. (23) by mass spectrometry. In 1973, Menaché and Girard [45] sampled water from the spring from which the specimens for the BIPM measurements were supplied about a century ago, and measured its isotopic composition. Assuming that the isotopic composition of the spring had not changed since the end of the nineteenth century and that the isotopic changes in the purification process had been reproduced correctly in their measurement, the density value converted for SMOW at 4 °C and 101.325 kPa was

$$\rho_{\text{SMOW}} \text{ (provisional)} = 999.975 \text{ kg/m}^3. \quad (24)$$

This value is provisional because no absolute density

measurement has been provided on the water they sampled.

4.2. Absolute measurement In 1994, an absolute density measurement for SMOM was first completed at the CSIRO [46], where the volume of a hollow sphere made of ultra low expansion glass was determined by optical interferometry, and the density of water was determined by the hydrostatic weighing of the sphere. The density of SMOW thus determined at 4 °C and 101.325 kPa was

$$\rho_{SMOW} (CSIRO) = 999.9736(9) \text{ kg/m}^3, \qquad (25)$$

where the numerical value in the parentheses expresses the combined standard uncertainty.

In 1996, an independent absolute density measurement for SMOW was completed at the NMIJ [47], where the volume of a fused quartz sphere was determined by an optical interferometer especially designed for a transparent sphere [48]. Hydrostatic weighing of the sphere in purified tap water and comparisons of the density of the tap water with that of purified water sampled from a deep ocean determined the density of SMOW at 4 °C and 101.325 kPa as

$$\rho_{SMOW} (NMIJ) = 999.9757(8) \text{ kg/m}^3, \qquad (26)$$

where the numerical value in the brackets expresses the combined standard uncertainty.

Although the absolute and independent density measurements on SMOW were carried out by the CSIRO and the NMIJ, their relative difference is as large as 2.1×10^{-6}, exceeding their combined standard uncertainties. For determining a new table for the density of SMOW, these data were statistically analyzed by the Task Group on the Density of Water organized in the CCM. The following value [49] was deduced for the density of SMOW at 4 °C and 101.325 kPa:

$$\rho_{SMOW} (CIPM) = 999.9749(4) \text{ kg/m}^3, \qquad (27)$$

where the numerical value in the brackets expresses the standard uncertainty. This value is recommended by the CIPM for the maximum density of SMOW at 101.325 kPa. The density of SMOW at temperatures in the range 0-40 °C is given also in [49], as well as a formulation for expressing the density as a function of temperature.

It should be stated that the value in Eq. (27) applies only to SMOW so that the density of a water sample must be calculated from Eq. (23). When we use distilled tap water, its density is usually less than that of SMOW by a few parts in 10^6. Its accurate density value can be obtained only when the isotopic composition of the sample is identified by mass spectrometry. Furthermore, dissolved gasses in water reduce its density. When air is dissolved in water at a saturated condition, the relative density reduction is about 4.6×10^{-6} at 0 °C. The effect of the dissolved air is also given in [49].
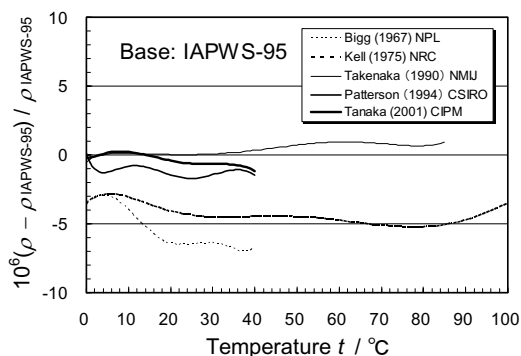

Fig. 8. Comparison of the density of water reported in different references. Bigg (1967) NPL: [51], Kell (1975) NRC: [52], Takenaka (1990) NMIJ: [53], Patterson (1994) CSIRO: [46], Tanaka (2001) CIPM: [49].

4. 3. Comparison Figure 8 compares the densities of water reported in different references. For convenience, the density calculated from IAPWS-95 [50] is used as a reference in this comparison. The values obtained from the CIPM formulation [49] agree with those from IAPWS-95 with relative differences of less than 1×10^{-6}. As for the table reported by Bigg [51] and for the formulation reported by Kell [52], they show a systematic relative difference of about 3×10^{-6} because their values are not corrected for the isotopic abundances. The values obtained from the formulation reported by Takenaka and Maui [53], which reproduces the density of SMOW at temperatures in a range 0-85 °C, agree with those from IAPWS-95 with relative differences of less than 1×10^{-6}. The values reported by Patterson and co-workers [46] show relative differences of less than 2×10^{-6}. These results suggest that the CIPM formulation [49] is reliable enough to express the density of SMOW at temperatures in the range 0-40 °C. If a wider temperature range, such as 0-100 °C, is needed for calculating the density of SMOW, IAPWS-95 may be used as a reliable formulation.

In the meeting of the CCM Working Group on Density (K. Fujii, Chairman) held at the BIPM in 2002, the progress of a new absolute measurement of the density of SMOW was reported by the Physikalisch-Technische Bundesanstalt (PTB) [54]. When the new data are available for the density of water, they will be evaluated, and a better formulation for expressing the density of water in a wider temperature range may be recommended by the CCM WG on Density.

5. Discussions
The development of the silicon sphere and the improvement in the optical interferometer have substantially reduced the uncertainty in the absolute density measurement, achieving a relative combined standard uncertainty of as small as 6.5×10^{-8}. In order

to change the present definition of the kilogram by the number of atoms or by the fundamental physical constants [55], a reduction of uncertainty by an order of magnitude is still needed. For example, the 94 mm diameter of the 1-kg silicon sphere must be known with an uncertainty of 0.3 nm to achieve a relative combined standard uncertainty of 1×10^{-8} in the density measurement. At this level, improved measurement technologies for surface properties will be needed, as well as the improvement in the optical interferometer to measure the diameter of the silicon spheres.

As for the differential density measurements, a relative combined standard uncertainty of 4.5×10^{-8} was already achieved by the hydrostatic weighing and pressure-of-flotation methods. When they are further improved and combined with a new absolute standard, a relative combined standard uncertainty of 1×10^{-8} may be achieved in the future. The technologies thus developed for the silicon density standard are already used at many NMIs for calibrating the densities of solids and fluids, contributing for founding a traceability of the density measurements used in science and industry.

References

[1] *The International System of Units (SI)*, 7th edition (Sèvres, Bureau International des Poids et Mesures, 1998).

[2] T. J. Quinn, *IEEE Trans. Instrum. Meas.*, **40**, 81-85 (1991).

[3] G. Girard, *Metrologia*, **31**, 317-336 (1994).

[4] T. j. Quinn, *Metrologia*, **36**, 211-244 (1999).

[5] J. B. Saunders, *J. Res. Natl. Bur. Stand.*, C **76**, 11-20 (1972).

[6] H. A. Bowman, R. M. Schoonover, and C. L. Carroll, *J. Res. Natl. Bur. Stand.*, A **78**, 13-40 (1974).

[7] R. D. Deslattes, A. Henins, H. A. Bowman, R. M. Schoonover, C. L. Carroll, I. L. Barnes, L. A. Machlan, L. J. Moore, and W. R. Shields, *Phys. Rev. Lett.*, **33**, 463-466 (1974).

[8] R. D. Deslattes, A. Henins, R. M. Schoonover, C. L. Carroll, and H. A. Bowman, *Phys. Rev. Lett.*, **36**, 898-900 (1976).

[9] A. J. Leistner and G. Zosi, *Appl. Opt.*, **26**, 600-601 (1987).

[10] A. J. Leistner and W. Giardini, *Metrologia*, **31**, 231-243 (1994).

[11] K. Fujii, M. Tanaka, Y. Nezu, K. Nakayama, R. Masui, and G. Zosi, *Rev. Sci. Instrum.*, **63**, 5320-5325 (1992).

[12] K. Fujii, M. Tanaka, Y. Nezu, A. Leistner, and W. Giardini, *IEEE Trans. Instrum. Meas.*, **44**, 542-545 (1995).

[13] D. P. Johnson, *J. Res. Natl. Bur. Stand.*, A **78**, 41-48 (1974).

[14] K. Fujii, M. Tanaka, Y. Nezu, K. Nakayama, H. Fujimoto, P. De Bièvre, and S. Valkiers, *Metrologia*, **36**, 455-464 (1999).

[15] A. Sakuma, K. Fujii, and M. Tanaka, *Meas. Sci. Technol.*, **5**, 1233-1238 (1994).

[16] N. Kuramoto and K. Fujii, *IEEE Trans. Instrum. Meas.*, **52**, 631-635 (2003).

[17] M. Born and E. Wolf, *Principles of Optics* , 6th edition (Oxford, Pergamon Press, 1980), Chap. 13, pp. 632-633.

[18] R. M. A. Azzam and N. M. Bashara, *Ellipsometry and Polarized Light* (Amsterdam, North-Holland, 1987), Chap. 4, pp. 283-288.

[19] D. F. Edwards, in *Handbook of Optical Constants of Solids*, ed. E. D. Palik (Orlando, Academic Press, 1985), Subpart 2, pp. 547-569.

[20] S. Mizushima, M. Ueki, and K. Fujii, *Metrologia*, **41**, S68-S74 (2004).

[21] K. Fujii, A. Waseda, N. Kuramoto, S. Mizushima, S. Valkiers, P. Taylor, and P. De Bièvre, *IEEE Trans. Instrum. Meas.*, **52**, 646-651 (2003).

[22] H. J. McSkimin and P. Andreatch, *J. Appl. Phys.*, **35**, 2161-2165 (1964).

[23] J. F. Nye, *Physical Properties of Crystals* (Oxford, Oxford University Press, 1992), Chap. 8, pp. 145-147.

[24] K. G. Lyon, G. L. Salinger, C. A. Swenson, and G. K. White, *J. Appl. Phys.*, **48**, 865-868 (1980).

[25] M. Okaji, *Int. J. Thermophys.*, **9**, 1101-1109 (1988).

[26] K. Fujii, A. Waseda, and N. Kuramoto, *Meas. Sci. Technol.*, **12**, 2031-2038 (2001).

[27] K. Fujii, *Metrologia*, **41**, S1-S15 (2004).

[28] A. Waseda and K. Fujii, *IEEE Trans. Instrum. Meas.*, **50**, 604-607 (2001).

[29] A. Waseda and K. Fujii, *Meas. Sci. Technol.*, **12**, 2039-2045 (2001).

[30] A. Waseda and K. Fujii, *Metrologia*, **41**, S62-S67 (2004).

[31] J. W. Beams and A. M. Clarke, *Rev. Sci. Instrum.*, **33**, 750-753 (1962).

[32] W. Wagner and R. Kleinrahm, *Metrologia*, **41**, S24-S39 (2004).

[33] R. Kleinrahm and W. Wagner, *J. Chem. Thermodyn.*, **18**, 739-760 (1986).

[34] N. Kuramoto, K. Fujii, and A. Waseda, *Metrologia*, **41**, S84-S94 (2004).

[35] C. Guillaume, *Trav. Mem. Bur. Int. Poids et Mesures*, **14**, 1-276 (1910).

[36] P. Chappuis, *Trav. Mem. Bur. Int. Poids et Mesures*, **14**, 1-163 (1910).

[37] J. Macé de Lépinay, J. H. Buisson, and J. R. Benoit, *Trav. Mem. Bur. Int. Poids et Mesures*, **14**, 1-127 (1910).

[38] C. Guillaume, *La Creation du B.I.P.M. et Son Oeuvre* (Paris, Gauthier-Villars, 1927).

[39] E. Cohen, K. M. Crowe, and J. W. M. Dumond, *The Fundamental Constants of Physics* (New York, Interscience Publishers, 1957).

[40] H. Craig, *Science*, **133**, 1833-1834 (1961).

[41] R. Hagemann, G. Nief, and E. Roth, *Tellus*, **22**, 712-715 (1970).

[42] R. Weast, *Handbook of Chemistry and Physics* (Cleveland, Ohio, Chemical Rubber, 1972).

[43] G. Kell, *J. Phys. Chem. Ref. Data*, **6**, 1109-1131 (1977).

[44] G. Girard and M. Menaché, *Metrologia*, **7**, 83-87 (1971).

[45] M. Menaché and G. Girard, *Metrologia*, **9**, 62-68 (1973).

[46] J. Patterson and E. C. Morris, *Metrologia*, **31**, 277-288 (1994).

[47] R. Masui, K. Fujii, and M. Takenaka, *Metrologia*, **32**, 333-362 (1995/96).

[48] K. Fujii, R. Masui, and S. Seino, *Metrologia*, **27**, 25-31 (1990).

[49] M. Tanaka, G. Girard, R. Davis, A. Peuto, and N. Bignell, *Metrologia*, **38**, 301-309 (2001).

[50] W. Wagner and A. Pruß, *J. Phys. Chem. Ref. Data*, **31**, 387-535 (2002).

[51] P. H. Bigg, *Brit. J. Appl. Phys.*, **18**, 521-525 (1967).

[52] G. S. Kell, *J. Chem. Eng. Data*, **20**, 97-105 (1975).

[53] M. Takenaka and R. Masui, *Metrologia*, **27**, 165-171 (1990).

[54] H. Bettin, presented in the meeting of the CCM Working Group on Density, BIPM, 2002.

[55] B. N. Taylor and P. J. Mohr, *Metrologia*, **36**, 63-64 (1999).